Taylor & Francis
Taylor & Francis Group

Measurement-based updating of turbine blade CAD models: a case study

MIHAILO RISTIC, DJORDJE BRUJIC and IAIN AINSWORTH

Abstract. Manufacturing industries, especially the aerospace and the automotive, require updating of CAD models so that the manufactured geometry is accurately represented. Often, additional constraints such as continuity are imposed on the model. The updated model may be employed to provide a more realistic analysis of the part's in-service performance. The necessary tools for realizing this task included dimensional measurement and geometric modelling. This paper discussed how this was achieved in the case of an aeroengine gas turbine blade. Measurement was performed using a coordinate measuring machine equipped with a touch trigger probe. Measurement path plan is based on the pre-processed CAD model. The accuracy was improved using our method for probe radius compensation. The re-modelling steps include preparation of the base surface, registration and least squares surface fitting. The surface preparation is needed in order to maintain prescribed continuity. Also, special attention was paid to cure ill-conditioning, which occurs when fitting trimmed surfaces. The adopted novel solution involves regularization and introduces two additional terms in the fitting functional. Two weighting coefficients are introduced to improve flexibility of the solution and they represent the user's confidence in the measurements and quality of the initial model.

1. Introduction

The manufacturing industry continues to face ever increasing pressures to reduce development lead times and to maximize performance and quality of their products. Especially demanding is the design and manufacture of complex parts comprising free-form geometry, such as those found in the aerospace and the automotive sectors. Development of such products relies extensively on the use of modern software tools for geometric design (CAD), engineering analysis (finite element analysis, computational fluid dynamics, etc.) and manufacture (CAM). These tools are used by dedicated specialist teams who are responsible for specific aspects of engineering design, in-service performance and manufacturing process development (Pahk *et al.* 1995). There is a continuing need to realize a higher level of integration between these activities (figure 1) in order to reduce the number of design iterations, minimize the need for experimental testing and on that basis to reduce the overall development timescales and costs.

In the case of high-performance, free-form components such as aeroengine compressors and turbine blades, it is generally difficult to relate the in-service performance to the specified manufacturing tolerances. Furthermore, these parts often do not possess clearly defined reference features and this makes it difficult to correlate the shape of the finished part with the design. For these reasons it is highly desirable to perform accurate re-modelling of the manufactured part by updating the original CAD model, which would provide an accurate representation of the manufactured geometry while preserving the design constraints imposed on the original model. The updated model may then be used to provide an input for the relevant simulation and analysis software tools, in order to better assess the actual performance of the component. By comparing these results with previous predictions and with the experimental performance data, one can obtain an invaluable insight into the component's in-service performance, improve the understanding of the manufacturing processes and also validate and further improve the simulation code itself.

Updating of *a priori* CAD models of free-form parts using point data poses several fundamental issues, including:

- maximizing the accuracy of the measurements and the updated model;
- dealing with large data sets of unorganized points, often involving measurement noise;

Authors: Mihailo Ristoc, Djordje Brujic and Iain Ainsworth, Department of Mechanical Engineering, Imperial College, Exhibition Road, London SW7 2BX, UK.

International Journal of Computer Integrated Manufacturing
ISSN 0951-192X print/ISSN 1362-3052 online © 2004 Taylor & Francis Ltd
http://www.tandf.co.uk/journals
DOI: 10.1080/0951192032000159148

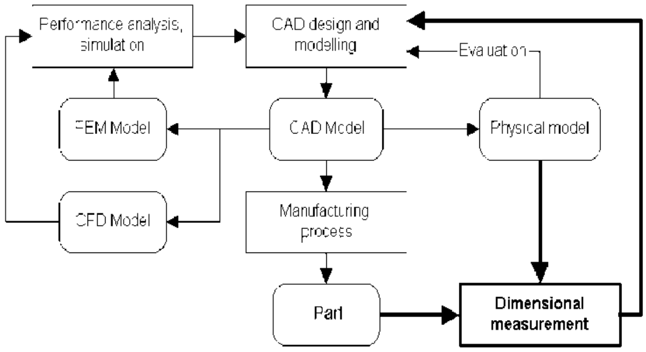

Figure 1. Contemporary framework for design and manufacture of free-form parts.

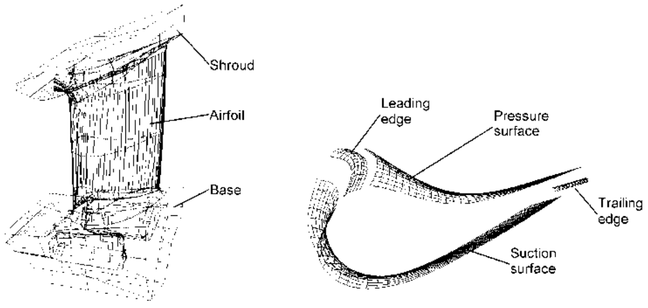

Figure 2. The CAD model of the complete turbine blade and an exploded view of the airfoil section indicating four constituent entities.

- dealing with complex CAD models comprising multiple, trimmed NURBS entities;
- maintaining the prescribed definition and surface continuity in the updated model.

The turbine blade application presented in this case study is considered to be highly representative of such requirements during product development and manufacture. Section 2 presents the detailed requirements in this application with an overview of the implemented method, while the subsequent sections deal with the implementation of specific steps of the process.

2. Overview of CAD model updating requirements and procedure

The turbine blade (figure 2) used in the case study was a part of a high-pressure stage of an aerospace gas turbine engine. Its CAD model was made available as an IGES file and consisted of over 1000 NURBS curve and surface entities. The gas washed surface of the blade, particularly the airfoil, represents the region of primary interest for measurement and updating.

The airfoil is composed of four distinct surfaces, corresponding to the suction side, the pressure side, leading and trailing edges. Importantly, the surfaces making up the airfoil are trimmed along the lines where they blend with the fillets that correspond to the base and the shroud of the blade.

2.1. *Model updating objectives*

The objective of the model updating exercise was to provide inputs for CFD analysis tools that would simulate the aerodynamic performance of the manufactured blade. In this work it was necessary to achieve compatibility with a number of CFD tools used for this purpose, including commercial packages for 3D flow analysis and programs specially developed for aerodynamic modelling of turbine blades. These programs posed a set of rigid rules for the definition of blade geometry, which were prescribed by the corresponding surfaces of the nominal CAD model.

One constraint was that the original parameterization of the airfoil surfaces was to be maintained in the updated model, in the sense that the start and end values of the knot vectors must be retained. This required appropriate reparameterizations to be performed at several stages of the updating process.

An important modelling constraint was that the updated airfoil surface must be curvature continuous. As will be shown in the subsequent sections, this was achieved by enforcing a C^2 continuity during merging, fitting and de-merging of the model entities. After the reparameterization undertaken in the final step, C^2 continuity is not guaranteed, but the required G^2 continuity is retained.

Thus the objective of model updating may be summarized as follows, to:

- update the nominal CAD model of the blade airfoil using dimensional measurements;
- maximize the overall accuracy;
- maintain the original number and type of constituent surfaces of the airfoil;
- maintain the original surface knot vector start and end values;
- maintain curvature continuity.

2.2. *Model updating method*

The overall method for model updating is shown in figure 3, which identifies the necessary processing tasks and the employed data. Model updating is

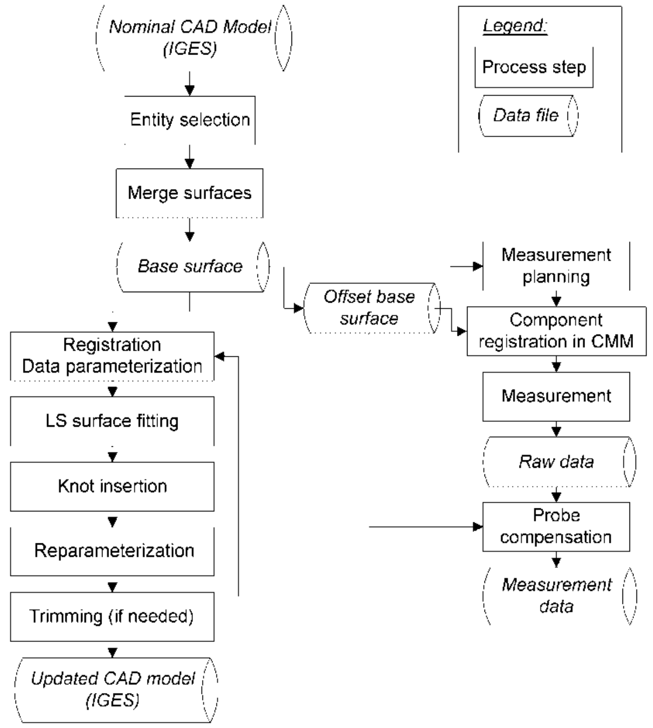

Figure 3. Outline of the CAD model updating process.

based on least squares surface fitting, requiring the use of a suitable base surface as the initial guess. In engineering applications such as this one, the base surface can be obtained from the nominal CAD model of the part, but in order to meet the specified requirements, it was necessary to pre-process that model through surface reparameterization and merging, as presented in section 5. In this way the required C^2 continuity was achieved as part of the surface fitting process.

The main steps in the model updating procedure may be summarized as follows.

(1) Preparation of the base surface using surface entities of the nominal CAD model.
(2) Measurement planning.
(3) Measurement execution and probe radius compensation.
(4) Registration, data parameterization.
(5) Least squares fitting.
(6) De-merging of entities, surface reparameterization and trimming (if needed).

The dimensional measurement task is an essential element of the updating process. For maximum accuracy, the measurements were performed using a coordinate measuring machine (CMM) equipped with a touch trigger probe. The key issues were identified to be measurement planning and probe radius compensation, both of which were resolved by employing the nominal CAD model, as presented in section 4.

Registration is an essential tool for establishing correspondence between the measured points and the model. It is also necessary to align the two since they are usually provided with respect to different coordinate frames. Registration is employed at two stages: as part of the measurement process to locate the component in the CMM and also in preparation for least squares surface fitting. The iterative closest point method (ICP) was adopted for this purpose (section 4).

Least squares fitting of NURBS surfaces deserves special attention, because the problem can easily become ill-posed due to an insufficient local density of the measured points in relation to the distribution of control points. This is critical in applications such as this one, where only a portion of the base surface is available for measurement and re-parameterization and knot insertion/removal also need to be applied. The adopted solution, presented in Section 5, is based on regularization and does not require re-measurement or interpolation of the measured data.

Following surface fitting, the final stage in the procedure involves post-processing of the updated model, without changing the shape, in order to present it precisely in the required form.

3. CAD modelling using NURBS

A NURBS surface of degree p in the u direction and degree q in the v direction is a bivariate vector-valued piecewise rational function of the form:

$$S(u,v) = \sum_{i=0}^{n}\sum_{j=0}^{m} R_{i,j}(u,v)P_{i,j} \qquad 0 \le u, v \le 1 \tag{1}$$

$$R_{i,j}(u,v) = \frac{N_{i,p}(u)N_{j,q}(v)w_{i,j}}{\sum_{k=0}^{n}\sum_{l=0}^{m} N_{k,p}(u)N_{l,q}(v)w_{k,l}} \tag{2}$$

where the control points $\{\boldsymbol{P}_{i,j}\}$ form a bi-directional control net and $\{w_{i,j}\}$ are control point weights. The functions $\{N_{i,p}(u)\}$ and $\{N_{j,q}(v)\}$ are the non-rational B-spline basis functions defined on the knot vectors

$$\begin{aligned} U &= \{\underbrace{u_{min},\ldots,u_{min}}_{p+1}, u_{p+1},\ldots,u_{r-p-1}, \underbrace{u_{max},\ldots,u_{max}}_{q+1}\} \\ V &= \{\underbrace{v_{min},\ldots,v_{min}}_{q+1}, v_{q+1},\ldots,v_{s-q-1}, \underbrace{v_{max},\ldots\ v_{max}}_{q+1}\} \end{aligned} \tag{3}$$

where $r = n + p + 1$, $s = m + q + 1$ and u_{min}, u_{max}, v_{min}, $v_{\max}$ are the end-knot values. Equations (1)–(3) define the evaluation of a point on a NURBS surface, the basic implementation of which is outlined in Piegl and Tiller (1997).

The above definition, with knot multiplicities $p + 1$ and $q + 1$ respectively at the edges, applies to NURBS surfaces which interpolate the end-points of their control polygon. Such NURBS are called clamped, or non-periodic. In contrast, NURBS with lower knot multiplicities at the edges do not interpolate the corresponding end-points of the control polygon and are referred to as *unclamped*, or *periodic* (Piegl and Tiller 1997). The terms clamped and unclamped are newer, more intuitive, and they are usually preferred in the CAD/CAM community, while the terms non-periodic and periodic are more often found in the literature. Although CAD models are primarily created using clamped surface entities, unclamped NURBS have an important role in modelling closed curves and surfaces.

3.1. *Trimmed NURBS*

A trimmed NURBS surface consists of a tensor product untrimmed NURBS surface and a set of trimming curves defined within the parameter rectangle of the surface (Piegl and Tiller 1997). The trimming curves are usually also NURBS, joined and properly ordered to represent outer boundaries and inner holes. Any number M_q of such curves can be expressed as:

$$C_q(t) = (u_q(t), v_q(t)) = \sum_{i=0}^{n} N_{i,k}(t)P_i^q \qquad q = 1, 2, \Lambda, M_q \tag{4}$$

with knot vectors:

$$\boldsymbol{T}_q = \{0, \ldots, 0, t_{k+1}, \ldots, t_{m-k-1}, 1, \ldots, 1\} \quad m = n + k + 1. \tag{5}$$

3.2. *Offset NURBS surface*

Offset NURBS surfaces are used extensively in the measurement phase (see section 6). They are specified by:

$$\mathbf{O}(u, v) = \mathbf{S}(u, v) + d\mathbf{N}(u, v) \tag{6}$$

where d is the offset distance. It has been proved (Piegl and Tiller 1998) that, given a NURBS surface $\mathbf{S}(u,v)$, its offset $\mathbf{O}(u,v)$ is generally not a NURBS. Therefore evaluation of an offset NURBS surface implies a degree of approximation. In this work, the offset surfaces were constructed using least squares fitting (section 5). The method first samples the original surface in the u and v directions, producing a regular grid. The minimum number of samples that has to be taken in order to construct the offset surface is one point per knot span, but it was found that using three points per knot span gave a good balance between speed and accuracy. Each sample point is then projected by a distance d in the direction normal to the surface. Once all of the offset points have been generated the offset surface can then be fitted in least squares fashion. The parameterization for the new surface is taken directly from the original one.

4. Registration

The adopted registration method involves least squares alignment of the measurement data with the surface entities of the nominal model. This was realized through an implementation of the ICP (iterative closest point) method (Besl and McKay 1992), which was reported by the authors in Ristic and Brujic (1997a) and verified in Ristic and Brujic (1997b). As the name suggests, the ICP method minimizes at each iteration step the collective square distances between the measured points and their closest points on the surface, defined by the cost function:

$$F = \sum_{i=1}^{M} |\boldsymbol{S}_i - \boldsymbol{R}\boldsymbol{Q}_i - \boldsymbol{t}|^2 \tag{7}$$

where $\boldsymbol{t}$ is the translation matrix, $\boldsymbol{R}$ is the rotation matrix, $\boldsymbol{Q}_i$ is the ith measurement point and $\boldsymbol{S}_i$ is the closest point on the nominal model and M is the number of measured points. In the implemented algorithm, the search for the nearest point on NURBS was realized using the multi-dimensional simplex method, while the least squares minimization was realized using singular value decomposition.

The ICP algorithm had been shown (Ristic and Brujic 1997b) to converge in the presence of measurement noise and for reasonable initial misalignments of several millimetres in position and several degrees in orientation. However, when the model and the part are initially grossly misaligned, convergence of the ICP algorithm cannot be guaranteed. For this reason it is necessary to bring the two closer together by some other means, as the first alignment step. This was achieved through a slight variant of the conventional corresponding point method. Simply, this means that six or more points are identified on the nominal model and then measured on the actual object by driving the

CMM manually. The corresponding points on the nominal surface are then aligned to the measured data in least squares fashion. Clearly the objective in this step is to align the two shapes only approximately, so it is not important that the two point sets correspond exactly. In our experience with a variety of engineering parts, this approach was found to produce sufficiently good initial alignment quickly, allowing full subsequent ICP registration to proceed.

It is also worth noting that the registration accuracy will be greatly increased if a large number of points is used for registration. It is therefore suggested that a larger number of points be used for ICP registration than for the initial alignment and to repeat this process once the full measurement data set is obtained.

5. Least squares fitting of NURBS surface

For a set of measured points $\{\boldsymbol{Q}_1,\ldots,\boldsymbol{Q}_M\}$, least squares fitting involves minimization of the collective square distance between those and their corresponding surface points, defined by the functional:

$$f=\sum_{k=1}^{M}|\boldsymbol{Q}_k-\boldsymbol{S}(u_k,v_k)|^2. \tag{8}$$

If the unknowns in the system are the control points, while the knot vectors, weights and parameters are set *a priori*, then the minimization problem will be linear. Parameterization, determining the values (u_k, v_k) for each measured point, is an important issue because it strongly influences the shape of the resulting surface. A number of parameterization methods have been published, but the majority of them make the assumption that the data are ordered. Since this work aims to deal with both ordered and unordered data, an alternative method was found following the suggestion in Ma and Kruth (1995), where parameterization can be achieved by projecting the points onto a base surface, from which the u_k and v_k values are obtained. In this application the required base surface can be obtained using the entities of the existing CAD model and the required parameterization is obtained as a result of registration.

The new positions of the control points are obtained as a solution of the system of normal equations (Dierckx 1993):

$$\boldsymbol{A}^{\mathrm{T}}\boldsymbol{A}\boldsymbol{a}=\boldsymbol{A}^{\mathrm{T}}\boldsymbol{b} \tag{9}$$

where $\boldsymbol{a}$ is a vector of $\boldsymbol{N}$ control points, $\boldsymbol{a}=[\boldsymbol{P}_{0,0}\ \ldots\ \ldots\ \boldsymbol{P}_{n,m}]^{\mathrm{T}}$; $\boldsymbol{b}$ is a vector of M measured points $\boldsymbol{b}=[\boldsymbol{Q}_1\ \ldots\ \ldots\ \boldsymbol{Q}_M]^{\mathrm{T}}$; and $\boldsymbol{A}$ is $M\times N$ matrix of coefficients of the points on the base surface that correspond to the measured points, defined by equation (2):

$$A=\underbrace{\begin{bmatrix} R_{0,0}(u_1,v_1) & \ldots & \ldots & R_{n,m}(u_1,v_1)\\ R_{0,0}(u_2,v_2) & & & R_{n,m}(u_2,v_2)\\ \vdots & & & \vdots\\ R_{0,0}(u_M,v_M) & \ldots & \ldots & R_{n,m}(u_M,v_M)\end{bmatrix}}_{N=(n+1)(m+1)}\Bigg\updownarrow M$$

The set of normal equations given by equation (9) may be solved by a number of methods, which can be broadly divided into direct ones, which require a fixed number of computations, and iterative ones. A suitable direct method is Cholesky factorization, but in common with all direct methods it is limited by the need to reserve memory for storing the matrix $\boldsymbol{A}^{\mathrm{T}}\boldsymbol{A}$. Thus for systems involving a large number of measured and/or control points, direct methods can become prohibitively expensive (De Boor 1993).

Such problems can be overcome by employing an iterative method, which starts from an initial approximation, which is successively improved until a sufficiently accurate solution is obtained. In this category, the method of successive displacements – the Gauss–Seidel method – computes a sequence of approximations $\boldsymbol{a}^{(1)}$, K, $\boldsymbol{a}^{(n)}$ where initial approximation $\boldsymbol{a}^{(0)}$ is assumed to be known (Press *et al.* 1993). Thus given $\boldsymbol{a}^{(a)}$ the method computes:

$$a_i^{(k+1)}=a_i^{(k)}+\frac{1}{N_{ij}}\Big(b_i-\sum_{j=1}^{i-1}N_{i,j}a_j^{(k+1)}-\sum_{j=1}^{n}N_{i,j}a_j^{(k)}\Big),\quad i=1,2,\ldots n. \tag{10}$$

The Gauss–Seidel method was adopted in this work for the solution phase. It also has the advantage that it leaves the matrix $\boldsymbol{A}^T\boldsymbol{A}$ unchanged throughout the process and allows its sparse and banded structure to be exploited. By storing and directly multiplying only the non-zero elements, the time and memory requirements can be drastically reduced.

5.1. *Ill-conditioning of the least squares problem and regularization*

It is quite easy for the matrix $\boldsymbol{A}^T\boldsymbol{A}$ in equation (9) to be ill-conditioned, or even rank deficient, and this becomes more likely as the system size increases. This problem arises from the local character of the basis functions and its detailed presentation is provided in Dierckx (1993). For the univariate case (curves), rank deficiency can be detected by examining validity of the

Shoenberg–Whitney conditions (Dierckx 1993), but such a simple test does not exist for the bivariate case (surfaces). Instead, De Boor shows (De Boor 1993) that $\boldsymbol{A}^T\boldsymbol{A}$ is positive definite and well-conditioned if there is at least one data point assigned to every knot span.

Ill-conditioning poses considerable problems in the context of CAD model updating. First, the NURBS surface entities of the CAD model, which provide the initial guess for the fitting, are often trimmed and some of their regions are not available for measurement. Second, knot insertion and/or reparameterization of the base surface are often required and this can also lead to insufficient measurement density in relation to the distribution of the control points in some regions. In Ma and He (1998) it is suggested that such problems may be alleviated by identifying the point deficient regions and excluding them from fitting. In addition, the point deficient regions may be re-measured, or the measured data may be interpolated to provide additional points where needed. However, none of these methods was found to be satisfactory in practice and the solution was sought through regularization of the linear system.

This problem has been analysed by the authors and a detailed presentation of the developed solution is provided in Brujic *et al.* (2002). It consists of including additional regularization criteria in the fitting functional (8), which were found to be well suited to the problem in hand and which guarantee that the least squares system is well posed. As a result, the fitting functional (8) is extended to include two additional terms, as follows:

$$f = \sum_{k=1}^{M} |\boldsymbol{Q}_k - \boldsymbol{S}(u_k, v_k)|^2 + \alpha \sum_{i=0}^{n}\sum_{j=0}^{m} \left|\boldsymbol{P}_{i,j} - \boldsymbol{S}(u_i^*, v_j^*)\right|^2 + \beta \sum_{i=0}^{n}\sum_{j=0}^{m} |\boldsymbol{P}_{i,j} - \boldsymbol{P}_{i,j}^0|^2. \quad (11)$$

The second term in the functional, with a weighting factor α, is introduced as a smoothing criterion and provides an equivalent of energy minimization. It minimizes the distance between the control points $\boldsymbol{P}_{i,j}$ and their corresponding Greville abscissae $\boldsymbol{S}(u_i^*, v_j^*)$. The Greville abscissae are the points on the surface at which the control points exercise the most influence and their parameters (u_i^*, v_j^*) are easily calculated by averaging of the knot values, such that $u_i^* = \frac{1}{p}(u_i + \ldots + u_{i+p})$ and $v_j^* = \frac{1}{q}(v_j + \ldots + v_{j+q})$ (Gordon and Riesenfield 1974).

The third term in equation (11), with a weighting factor β, has the effect to minimize the overall movement of the control points from their initial values $\boldsymbol{P}_{i,j}^0$. The inclusion of this term is important because it guarantees well-posedness of the system for $\beta > 0$, while in some applications it may also be employed to preserve the original shape of the regions that are not covered by the measurements.

The adoption of the functional (11) leads to a set of generalized normal equations:

$$\left[\boldsymbol{A}^T\boldsymbol{A} + \alpha(\boldsymbol{B}-\boldsymbol{I})^T(\boldsymbol{B}-\boldsymbol{I}) + \beta\boldsymbol{I}^T\boldsymbol{I}\right]\boldsymbol{a} = \boldsymbol{A}^T\boldsymbol{b} + \beta\boldsymbol{a}^0 \quad (12)$$

where **A, a** and **b** are as in equation (9), **I** is the identity matrix, **B** is the matrix of rational basis function values for the values of the parameters of the Greville points:

$$B = \begin{bmatrix} R_{0,0}(u_{0,0}^*, v_{0,0}^*) & \ldots & \ldots & R_{n,m}(u_{0,0}^*, v_{0,0}^*) \\ R_{0,0}(u_{0,0}^* v_{0,1}^*) & & & R_{n,m}(u_{0,1}^*, v_{0,1}^*) \\ \vdots & & & \vdots \\ R_{0,0}(u_{n,m}^*, v_{n,m}^*) & \ldots & \ldots & R_{n,m}(u_{n,m}^*, v_{n,m}^*) \end{bmatrix}$$

and $\boldsymbol{a}^0$ is the vector of the original control points:

$$\boldsymbol{a}^0 = \left[\boldsymbol{P}_{0,0}^0 \; \ldots \; \ldots \; \boldsymbol{P}_{n,m}^0\right]^T.$$

Equation (12) is solved using the same methods as those used for solving equation (9).

The weights α and β may be calculated according to the following expressions:

$$\alpha = \alpha' \frac{Tr(\boldsymbol{A}^T\boldsymbol{A})}{Tr((\boldsymbol{B}-\boldsymbol{I})^T(\boldsymbol{B}-\boldsymbol{I}))} \qquad \beta = \beta' \frac{Tr(\boldsymbol{A}^T\boldsymbol{A})}{Tr(\boldsymbol{I}^T\boldsymbol{I})} \quad (13)$$

where $Tr(.)$ denotes the sum of the diagonal elements (or trace) of a matrix, and α' and β' represent the user specified ratios between the weightings assigned to the smoothing α-term and the shape preserving β-term, respectively, in relation to that of the measurement term (Press *et al.* 1993).

The choice of the weighting ratios $\alpha' \geqslant 0$ and $\beta' \geqslant 0$ is important, as they influence the shape of the resulting surface, but there is no general technique that would always lead to optimal results (Brujic *et al.* 2002). In practice, these values are set by the user, based on the measurement characteristics and on the desired overall result. The main considerations in setting these values are:

- confidence in the measurements – accurate measurements would be assigned a higher relative weighting by using smaller values of α' and β', while noisy measurements demand more smoothing, achieved by a larger α';
- preservation of the shape of the unmeasured, or sparsely measured, regions – achieved with a larger β'.

In the work presented in this paper the choice of these weightings was guided primarily by the confidence in the measurements. The turbine blade measurements performed using the CMM and the adopted measurement procedure (section 6) were considered to be very accurate. For this reason the measurement term was assigned ten times the relative weighting of the smoothing term, by adopting the value $\alpha' = 0.1$. The unmeasured regions of the airfoil are those corresponding to the trimmed portions of the model surface, the shape of which was of no particular importance, other than the requirement to ensure a smooth blend between those and the updated regions (as realised by the α-term). For this reason the β-term was assigned a very small relative weighting $\beta' = 0.001$, in order to guarantee that the system is well posed, but with very little other effect on the shape of the updated surface. As will be shown in section 7, the weightings chosen on this basis produced highly satisfactory results.

6. Measurement

In order to maximize the overall precision, a conventional computer-controlled CMM equipped with a touch trigger probe was chosen as the measuring instrument for this application. This type of equipment was selected because it is capable of achieving measurement accuracy of a few microns. Other candidate instruments would include non-contact laser triangulation systems, but their measurement accuracy is typically an order of magnitude lower and they were considered to be inadequate for this application. Two aspects of the measurement process demanded special attention: probe radius compensation and measurement planning.

6.1. *Probe radius compensation*

With any contact measuring system, probe radius compensation can become a significant source of systematic error when dealing with free-form geometry (Ristic *et al.* 2001), as the system records the position of the probe tip centre (raw measurements), while the position of the actual point of contact needs to be derived by estimating the corresponding surface normal direction. The solution to this problem was found by employing offset surfaces of the nominal model, where the offset is equal to the probe radius. The offset surfaces are fitted (section 5) to the raw measurements and the required normal vectors are then calculated at the surface points corresponding to the raw data points. The corresponding points are found as part of the registration process.

6.2. *Measurement planning*

Explicit control of the measurement process was realized through measurement planning, which was carried out on the basis of the CAD model. Interactive graphical tools (Ainsworth *et al.* 2000) were developed and used to define the surface sampling points, generate a collision free probe path and verify the machine executable code before downloading to the CMM controller for execution. Figure 4 provides

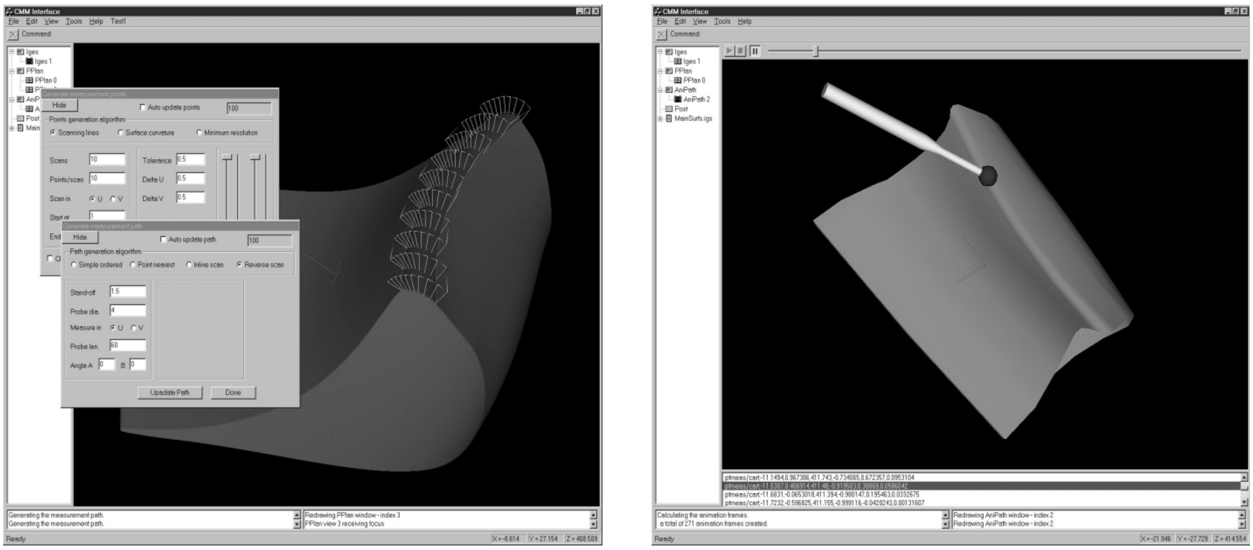

Figure 4. Measurement planning: (a) determining point distribution; and (b) measurement simulation.

sample screens shots of the path planning software being applied to the measurement of the turbine blade airfoil.

The measurement points are defined using adaptive subdivision sampling of the model surface. Several surface sampling criteria have been identified and implemented, to be employed by the user individually or in combination. These include:

- uniform sampling in the u and v parametric directions;
- chordal deviation criterion – sampling density is determined by the surface curvature;
- minimum sample density criterion – specifies the maximum allowed distance between neighbouring points;
- parameterization-based sampling criterion – sampling density is determined in relation to the knot vector of the model surface.

The parameterization-based criterion was found to be particularly important in this application, since the purpose of the measurement is to provide data for subsequent NURBS surface fitting. The quality of the fitted surface will be significantly improved by ensuring that there is at least one point situated within each knot span. This sampling criterion is therefore based on the model parameterization, with the required number of samples per knot span being specified by the user.

It should also be noted that the original CAD model of the blade had to be processed (see section 7) through merging and reparameterization of its constituent surfaces, in order to provide a suitable base surface for the subsequent fitting. Therefore it was this processed model that was employed for measurement planning.

6.3. *Overall measurement procedure*

Following the above description, the overall measurement procedure may be summarized as follows.

(1) Prepare the CAD model.
(2) Generate the offset nominal NURBS surface – the offset distance being that of the probe tip radius.
(3) Fix the blade in a suitable location within the CMM.
(4) Define and measure six corresponding points on the component and on the offset nominal surface.
(5) REGISTRATION STEP 1 – Using the six point pairs rotate and translate the nominal CAD model into an approximately correct position. Record the transformation matrix.
(6) Measure several tens of points at suitable positions, such that the movement of the object is constrained.
(7) REGISTRATION STEP 2 – Perform ICP registration between the measured points and the offset surface. Record the transformation.
(8) Perform measurement planning using the registered CAD model in order to generate the machine instructions necessary for full measurement.
(9) Perform measurement and record raw measurement points.
(10) REGISTRATION STEP 3 – Perform ICP registration using the full raw measurement set and the offset surface.
(11) Perform least squares fitting of the offset surface to the raw measurements.
(12) Calculate surface normal vectors at corresponding points and apply probe radius compensation to the raw measurements.

The output of the measurement process is therefore a set of 3D points measured on the object surface, which then provide the input for the re-modelling of the corresponding NURBS surfaces in the next step.

7. Turbine blade re-modelling

Following the presentation of the implemented methods for registration, measurement and surface fitting, we now describe how the overall procedure was carried out in the case of turbine blade re-modelling and we show the results. The first step in the process involved preparation of a suitable base surface using the original CAD model.

7.1. *Base surface preparation*

The nominal CAD model of the blade airfoil consisted of four distinct surface entities. The surface fitting procedure presented in section 5 may be applied to each surface in turn, but this would not meet the prescribed C^2 continuity conditions across the boundaries. Furthermore, the airfoil represents a wraparound surface and this poses further considerations. These problems were overcome essentially by merging the distinct NURBS entities of the nominal CAD model into one, performing the least squares surface fitting and then breaking the resulting surface into the required number of entities. It is important to note that in this case, when merging two entities, the position of all of the control points remains unchanged in space. The new matrix of control points and new knot vectors are obtained through re-grouping of the existing ones. This process is presented below.

7.1.1. *Merging surface entities.* All of the airfoil surface entities are clamped, meaning that for a surface degree p, the knot multiplicity corresponding to the end-points is $p + 1$. Merging two such entities results in an entity with a knot multiplicity equal to p along the curve where the surfaces are merged. However, for a NURBS of degree p, continuity C^2 is guaranteed only for knot multiplicity p - 2 or less. In the example airfoil considered here we had $p = 3$, meaning that the knot multiplicity had to be no more than 1 in order to preserve the required continuity after fitting. Consequently, the knot multiplicity had to be lowered and this was achieved through knot removal.

While knot insertion does not change the shape of the surface, the reverse process, knot removal, cannot be carried out, in general, without changing the shape. A detailed review of knot removal algorithms for NURBS curves can be found in Eck and Hadenfeld (1995). As pointed out by Lyche and Morken (1987) all control points are involved in the knot removal procedure. However, Sapidis (1990) suggested an elegant way of knot removal for curves, where the movement of control points is minimized. It is based on the following observation: if the continuity of a NURBS curve at the knot which is to be removed is higher than it should be according to its multiplicity, then this knot is only a pseudo knot, which could be removed from the knot sequence without changing the curve. Hence, the idea is to move the control points associated with the knot in question so that the resulting new curve becomes C_{p-s+1} continuous, where s is the knot multiplicity.

The algorithms for surface knot removal are quite complex. Without going into details, it is only pointed out that the knot u_r (or v_r) is removed from the surface by applying the curve knot removal algorithm suggested by Tiller (1992) to $n + 1$ columns (or $m + 1$ rows) of control points. However, for this procedure to work properly it is important that the ratio (knot span)/(corresponding arc length) remains approximately constant across the two merging entities. Otherwise, knot removal will cause a significant displacement of the control points. It can be seen from figure 5 that this ratio for adjacent airfoil entities was highly dissimilar (an order of magnitude difference in fact), necessitating reparameterization of these entities before merging. This was achieved through linear

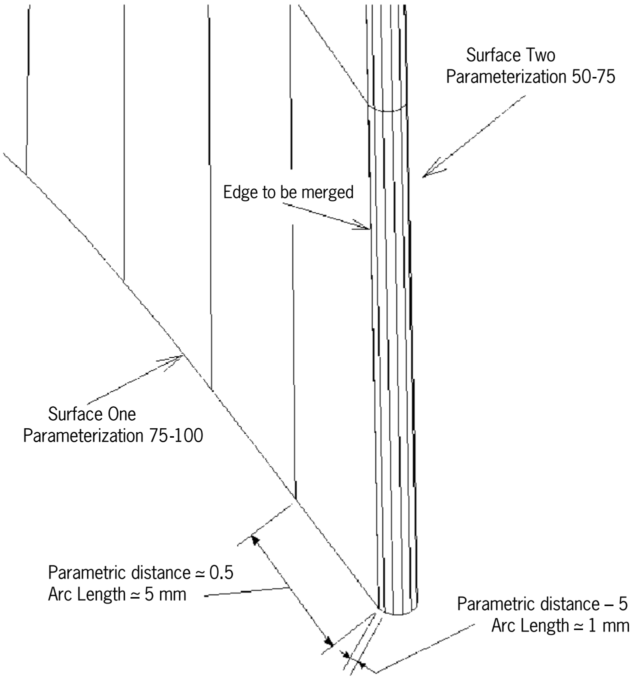

Figure 5. Initial parameterization.

reparameterization, which was realized according to the procedure presented in Piegl and Tiller (1997), with the effect of changing the parameter bounds $[u_{\min}, u_{\max}]$ and the corresponding scaling of knot values.

7.1.2. *Closed surface.* The application of the above reparameterization and merging procedure results in a single surface entity which is guaranteed to satisfy the C^2 continuity constraint everywhere, except at the line where the surface is closed (i.e. where the start and end edges meet). It is therefore necessary to account for the fact that the airfoil surface is closed in one parametric direction.

The solution is illustrated in figure 6 and it involves turning the non-periodic, clamped surface into a periodic, unclamped one, with wraparound of control points. Following the procedure presented in Piegl and Tiller (1997), unclamping is essentially equivalent to knot removal. Starting with a clamped surface of order p and knot multiplicity $p + 1$ at the edges, repeated knot removal produces an unclamped surface with edge knot multiplicity of one and $2p$ additional control points. This therefore leaves $2p$ additional knots, which may be chosen arbitrarily. If the end knots are chosen according to:

$$\begin{aligned} u_{p-i-1} &= u_{p-i} - (u_{n-i+1} - u_{n-i}) \quad i=0,\ldots,p-1 \\ u_{n+i+2} &= u_{n+i+1} + (u_{p+i+1} - u_{p+i}) \quad i=0,\ldots,p-1 \end{aligned} \tag{14}$$

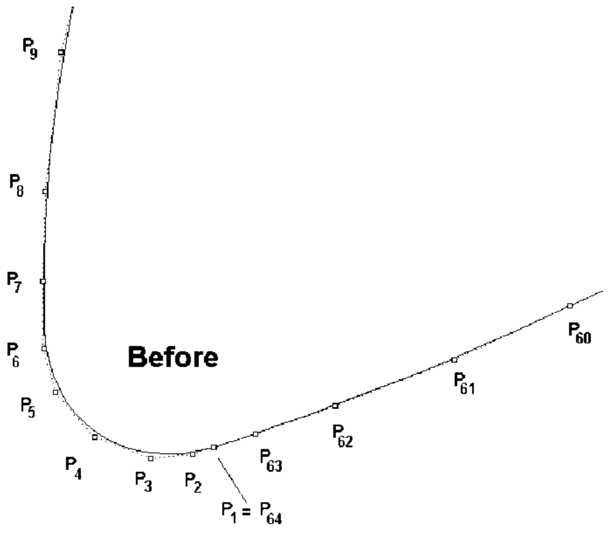

Figure 6. Unclamping.

then the result is a wraparound of the control points. As figure 6 illustrates, in this case $p = 3$ and this gives three pairs of identical control points.

The procedure for modelling closed curves presented in Piegl and Tiller (1997) was extended to deal with surfaces. The wraparound surface produced in this way is guaranteed to preserve the required C^2 continuity everywhere, because all knot multiplicities are equal to one (Farin 1997). Therefore by fitting this surface to the data points, while maintaining the wraparound of control points, the fitted surface will also maintain this constraint. The surface fitting algorithm outlined in section 5 needs only slight adjustments to cater for changes in indexing in order to fit the closed surface.

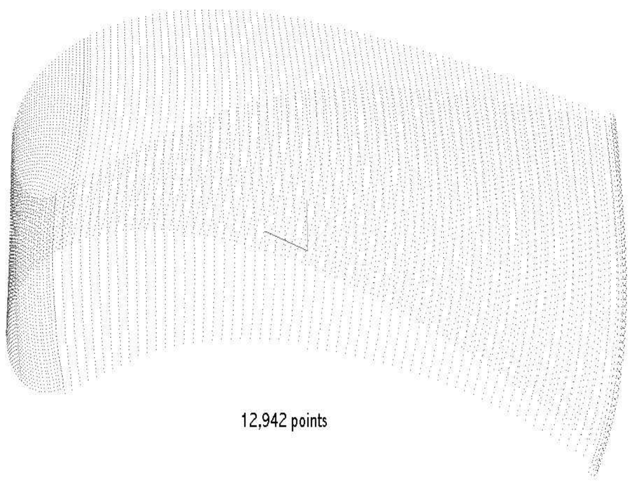

Figure 7. Measured points.

7.2. *Measurement*

The generated base surface was employed for measurement planning. The surface sampling density was controlled by the chordal deviation criterion (set to 1 μm) and by the parameterization-based criterion which ensured at least one sample point per knot span. The procedure outlined in section 6 was then applied to collect a set of just under 13 000 points using the CMM, as shown in figure 7.

The measurements were performed using a computer-controlled CMM, model LK G-90C, equipped with Renishaw PH-10 indexing head and Renishaw TP2-5W touch trigger probe. This equipment was verified to achieve measurement accuracy of 2–3 μm in obtaining the raw positional data (probe sphere centre positions) and this level of accuracy was maintained following the probe radius compensation, using the procedure outlined above.

7.3. *Model updating*

Least squares surface fitting method was applied with the relative settings of the weights $\alpha' = 0.1$ and $\beta' = 0.001$. As explained previously, this gave ten times higher weighting to the measurement term in relation to the smoothing term (Press *et al.* 1993, Farin 1997), because the CMM and the adopted measurement procedure were considered to provide very accurate measurements. In contrast, measurements obtained using non-contact systems based on laser light were from previous experience found to result in at least an order of magnitude lower accuracy and a noise characteristic that is highly dependent on the surface finish of the part.

The application of surface fitting produced the updated airfoil model as a single wraparound surface (figure 8). In the final step, it is necessary to restore the four entities of the airfoil through a reverse process of clamping, knot insertion, surface splitting and re-parameterization.

Figures 9 and 10 present an accuracy analysis of the final result. Figure 9 shows a display of errors between the measured data and the reconstructed model, with the average error under 4 μm. Figure 10 shows the comparison between the original and the updated CAD model, with the average error of 26 μm.

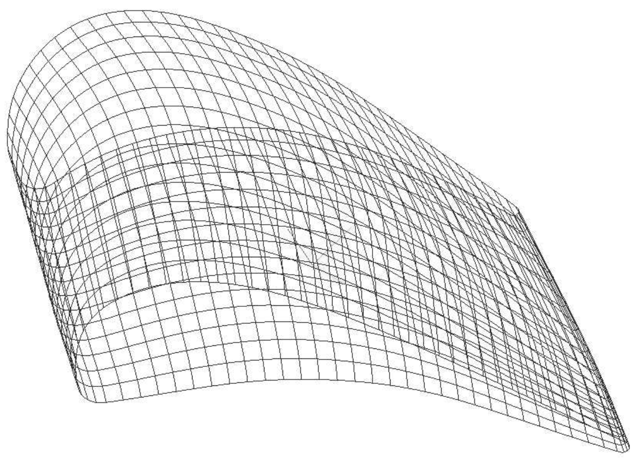

Figure 8. Reconstructed airfoil shape.

The final result of the process was exported as an IGES file. If required, the updated airfoil may be incorporated in the overall blade model by blending it with the base and shroud surfaces using fillets. This can be performed using an available CAD package, in principle by repeating such modelling steps that were previously used in the creation of the original model.

8. Conclusion

This paper has presented a method for measurement-based updating of turbine blade CAD models, as dictated by the requirements during product development and manufacture. The main requirements in this application involve maximizing the overall accuracy and maintaining the prescribed characteristics of the CAD model in terms of its composition from the constituent entities, parameterization and curvature continuity. When dealing with free-form precision engineering parts of this type, both the measurement and the geometric modelling aspects of the process need to be carefully addressed. The paper has presented how a combination of methods related to both of these aspects was employed to produce high-quality results that met all of the prescribed objectives.

The most novel element of the process is considered to be the implemented method for least squares fitting of NURBS, which makes no special assumptions about the measurement distribution. Unlike other such methods proposed in the literature it does not require exclusion of certain regions from the fitting, re-measurement nor interpolation of the measured data. This was achieved by the adoption of the regularization

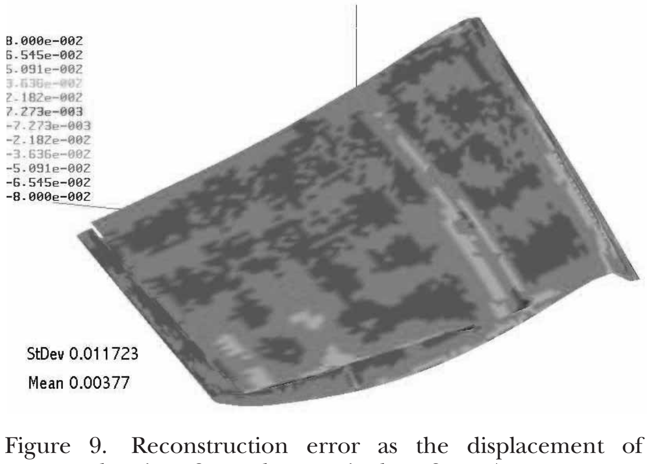

Figure 9. Reconstruction error as the displacement of measured points from the nominal surface. (average error under 4 μm)

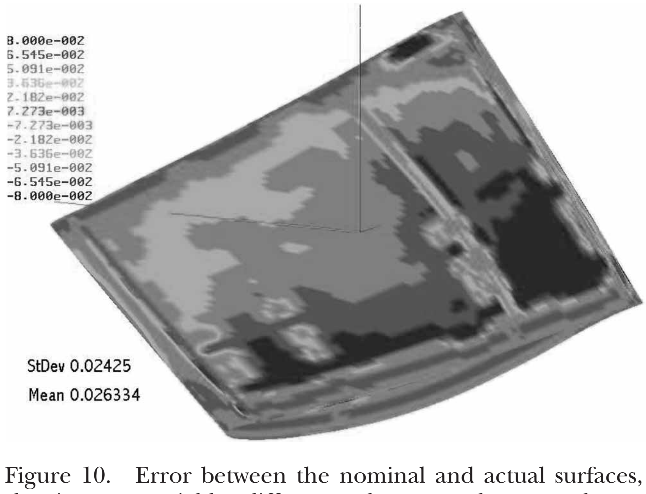

Figure 10. Error between the nominal and actual surfaces, showing appreciable difference between the two shapes (average error around 26 μm).

criteria that are well suited for the problem in hand and provide a sufficient control over the quality of the fitted shape. The corresponding weighting factors may be selected according to a number of criteria, the most important being the user's confidence in the measured data.

The surface fitting method was employed at two stages of the updating process: to calculate the offset surface of the nominal model as a basis for accurate probe radius compensation and to produce the updated CAD model of the component. The paper also presented how the prescribed curvature continuity and other modelling requirements were met through appropriate preparation of the base surface, for which a number of geometric modelling functions were implemented and employed.

The experience gained in this work has also highlighted the importance of performing dimensional measurements that are optimized for the task in hand and for the adopted measuring instrument. The implemented tools for CAD-based measurement planning and execution are considered to be essential for achieving high-quality results.

Acknowledgements

This work has been partly supported by the Engineering and Physical Science Research Council grants GR/N11285 and GR/M/87351.

References

Ainsworth, I., Ristic, M., and Brujic, D., 2000, CAD-based measurement path planning for free-form shapes using contact probes. *International Journal of Advanced Manufacturing Technology*, **16,** 23–31.

Besl, P. J., and McKay, N. D., 1992, A method for registration of 3-D shapes. *IEEE Trans. on Patt. Ann. and Mach. Intel.*, **14**(2), 239–256.

Brujic, D., Ristic, M., and Ainsworth, I., 2002, Measurement-based modification of NURBS surfaces. *Computer Aided Design*, **34**(3), 173–266.

De Boor, C., 1993, Gauss elimination by segments and multivariate polynomial interpolation. Purdue Conference on Approximation and Computation, West Lafayette, IN: 1993.

Dierckx, P., 1993, *Curve and Surface Fitting with Splines* (Oxford: Clarendon).

Gordon, W., and Riesenfield, R., 1974, B-spline curves and surfaces. In Barnhill and Riesenfield (eds). *Computer Aided Geometric Design* (New York: Academic Press), pp. 95–125.

Eck, M., and Hadenfeld, J., 1995, Knot removal for B-spline curves. *Computer Aided Geometric Design*, **12,** 259–282.

Farin, G. E., 1997, *Curves and Surfaces for Computer-aided Geometric Design: a Practical Guide,* 4th edn (New York: Academic Press).

Lyche, T., and Morken, K., 1987, Knot removal for parametric B-spline curves and surfaces. *Computer Aided Geometric Design*, **4,** 217–230.

Ma, W., and He, P. R., 1998, B-spline surface local updating with unorganised points. *Computer Aided Design*, **30**(11), 853–862.

Ma, W., and Kruth, J. P., 1995, Parameterization of randomly measured points for least squares fitting of B-spline curves and surfaces. *Computer-Aided Design*, **27**(9), 663–675.

Pahk, H. J., Jung, M. Y., Hwnag, S. W., Kim, Y. H., Hong, Y. S., and Kim S. G., 1995. Integrated precision inspection system for manufacturing of moulds having CAD defined features. *The International Journal of Advanced Manufacturing Technology*, **10**(3), 98–207.

Peterson, J. W., 1994, Tessellation of NURBS Surfaces. In P. S. Heckbert (ed.) *Graphic Gems IV* (New York: Academic Press), pp. 287–319.

Piegl, L. A., and Richard, A. M., 1995, Tessellating trimmed NURBS surfaces. *Computer Aided Design*, **27**(1), 16–26.

Piegl, L. A., and Tiller, W., 1997, *The NURBS Book*, 2nd edn (New York: Springer).

Piegl, L. A., and Tiller, W., 1999, Computing offsets of NURBS curves and surfaces. *Computer Aided Design*, **31,** 147–156.

Press, W. H., Teukolsky, S. A., Vetterling, W. T., and Flannery, B. P., 1993, *Numerical Recipes in C: The Art of Scientific Computing,* 2nd edn (Cambridge: Cambridge University Press).

Ristic M., Ainsworth, I., and Brujic, D., 2001, CAD-based CMM probe radius compensation for free-form surfaces. Proceedings I. Mech. Eng. Part B, Journal of Engineering Manufacture.

Ristic, M., and Brujic, D., 1997a, Efficient registration of NURBS geometry. *International Journal of Image and Vision Computing*, **15,** 925–935.

Ristic, M., and Brujic, D., 1997b, Analysis of free form surface registration. *Proceedings Institution of Mechanical Engineers*, **211**(Part B), 605–617.

Sapidis, N., and Farin, G., 1990, Automatic fairing algorithm for B-spline curves. *Computer Aided Design*, **12,** 73–77.

Tiller, W., 1992, Knot-removal algorithms for NURBS curves and surfaces. *Computer Aided Design*, **24**(8), 445–453.